Dissociation of Hydrogen Chloride and Proton Transfer in Liquid Glycerol: An Ab Initio Molecular Dynamics Study†

Wei Zhuang and Christoph Dellago*

Department of Chemistry, University of California at Irvine, Irvine, California 92697, and Faculty of Physics, University of Vienna, Boltzmanngasse 5, 1090 Vienna, Austria

Received: May 28, 2004; In Final Form: August 10, 2004

The dissociation and recombination of hydrochloric acid in bulk liquid glycerol under ambient conditions is studied with ab initio simulations. In two different molecular dynamics trajectories HCl dissociation occurred within a few picoseconds, a time scale consistent with recent molecular beam experiments. The dissociation of the hydrochloric acid molecule is initiated by the formation of additional hydrogen bonds accepted by the chloride ion. The subsequent separation of the nascent ions occurs via the diffusion of a protonic defect along chains of hydrogen bonds in a Grotthus-like fashion.

I. Introduction

The dissociation and dissolution of acids in and on polar substances plays an important role in many processes in nature and technology. For example, the dissociation of hydrogen chloride on ice particles in stratospheric clouds is central to the chlorine chemistry involved in polar ozone depletion.[1,2] Recent theoretical work has focused on the ionization of hydrochloric acid in bulk water,[3−5] in small water clusters,[6−8] and on the surface of ice.[9−14] These studies revealed that HCl ionizes in such aqueous systems provided the HCl molecule is coordinated by three water molecules. In bulk water, a low dissociation barrier related to a collective solvent reorganization[5] leads to rapid, subpicosecond dissociation of the HCl molecule followed by Grotthus diffusion of the liberated proton.[3]

Similar processes are expected to take place in other polar, hydrogen-bonded solvents such as glycerol, $HOCH_2CH(OH)CH_2OH$. In a series of recent molecular beam scattering experiments, Nathanson and co-workers studied the interactions of HCl (and HBr) molecules with the surface of liquid glycerol.[15,16] Glycerol has a rich phase behavior due to its complex hydrogen bonding structure[17] and is an excellent glass former[18,19] acting as a natural cryoprotectant.[20] The low vapor pressure of glycerol makes it possible to maintain a sufficiently good vacuum over the liquid such that incoming HCl molecules can reach the surface before colliding with a molecule in the vapor phase. Due to its high dielectric constant ($\epsilon = 41$) and its hydrogen bonding properties liquid glycerol has some similarities with liquid water (the viscosity of glycerol, however, exceeds that of water by many orders of magnitude). Though earlier molecular dynamics simulations based on empirical force fields[22] indicate that on the average each molecule donates (and accepts) 1.7 intermolecular and 0.08 intermolecular hydrogen bonds, we find higher hydrogen bond numbers (2.85 intermolecular and 0.4 intramolecular hydrogen bonds) in our ab initio simulations, as discussed later. The diffusion constant of protonic defects[23] is much higher than the self-diffusion constant of glycerol molecules,[24] suggesting that excess protons diffuse along the network of hydrogen bonds according to the Grotthus mechanism observed in water[25−29] and other hydrogen-bonded liquids such as methanol[30] and hydrogen fluoride.[31]

From their molecular beam experiments,[15,16] Nathanson and co-workers were able to determine probabilities and estimate time scales for various processes following the collision of the HCl molecules with the glycerol surface. HCl molecules impinging on the glycerol surface with an angle of 45° are trapped and thermalize in the interfacial region with a probability of 0.6−0.9 depending on the incident energies. Though more than 70 of the trapped HCl molecules penetrate into the bulk liquid and dissociate, the remaining molecules desorb into the gas phase on a time scale shorter than 10^{-6} s. Surprisingly, about a quarter of these HCl molecules temporarily trapped on the surface undergo hydrogen exchange before they desorb. Although the experiments yield detailed statistical information on the processes occurring after the HCl molecules strike the liquid−gas interface, they are not capable of resolving the mechanisms on a microscopic level. It is, for instance, unclear at which depth and on which time scales HCl molecules dissolving into the bulk liquid ionize. Furthermore, the experiments are consistent with different mechanisms for the immediate hydrogen exchange in the interfacial region. This reaction can either occur via the dissociation of the HCl molecule and subsequent hydrogen exchange followed by recombination or through a concerted and neutral bond switching mechanism involving the HCl molecule and OH groups of the solvating glycerol molecules.[16]

Computer simulations can provide the microscopic information needed for the interpretation of the empirical data obtained from such molecular beam experiments. In a recent molecular dynamics study, Chorny, Benjamin, and Nathanson have shed light on the early stages of the HCl−glycerol interaction following a surface collision.[33] The scattering and trapping probabilities as well as the energy loss of the scattered molecules obtained from these simulations agree well with the experimental results. Free energy profiles as a function of the HCl bond length indicate that formation of a contact ion pair is facile, involving a dissociation barrier of about 2 kcal/mol both in the bulk as well as in the interfacial region. Perhaps most relevant for the interpretation of the experiments, dissociation to the ion pair is found to take place in the interfacial region (at less than 4 Å of

† Part of the special issue "Frank H. Stillinger Festschrift".

10.1021/jp047676r CCC: $27.50 © 2004 American Chemical Society
Published on Web 10/30/2004

depth) and to occur within 5 ps after collision with the surface. These results provide additional evidence for the possibility of a proton exchange reaction in the surface region, as suggested by the experiments of Ringeisen et al.[16]

Although the simulations by Chorny et al.[33] yield detailed information about the scattering off the surface and the early stages of HCl dissociation up to the contact ion pair, the model on which these simulations are based is not capable of describing the entire dissociation reaction including the formation of a solvent separated ion pair and the complete separation of the ionization products. The reason is that the specific empirical valence bond model[34−38] developed for this system[33] does not include a description of proton transfer between glycerol molecules.

Ab initio molecular dynamics simulation offers an alternative approach to this problem.[39] Although computationally expensive, density functional theory (DFT) based computational techniques such as Car−Parrinello molecular dynamics[40] are capable of describing structure and dynamics of bond breaking and formation. Limited only by the approximations of DFT and of the classical propagation of the nuclear degrees of freedom, Car−Parrinello molecular dynamics can be used to describe chemical processes in an essentially parameter free way. Here, we report on the application of Car−Parrinello molecular dynamics to the dissociation of an HCl molecule in liquid glycerol. Though our system is small (it consists of 15 glycerol molecules plus one HCl molecule), periodic boundary conditions ensure that our results are relevant for the bulk phase. Naturally, similar studies near the liquid−gas interface would be desirable, but we postpone them for later studies due to the larger computational cost of such simulations compared to bulk simulations.[41] Our dissociation simulations are complemented with Car−Parrinello molecular dynamics studies of neat glycerol and the solvation and transport of an excess proton in liquid glycerol as it occurs following the ionization of an HCl molecule.

Anticipating our main results, we find that the ionization occurs on a picosecond time scale, about an order of magnitude slower than in liquid water.[3] The ionization process appears to be driven by a reorganization of the solvation structure around the dissociating HCl molecule. After dissociation the proton hops along hydrogen bonds between glycerol molecules. Although the motion along such wires is rapid, occurring on a subpicosecond time scale, the proton visits only a short segment of a longer hydrogen bond chain. The reasons for this effective proton confinement are presently unknown and will be the subject of future studies. The time scales for HCl dissociation observed in our simulations are consistent with those found in the simulations of Chorny et al.[33] and with the experiments of Ringeisen et al.[15,16]

The remainder of the paper is organized as follows. After delineating the computational methods in section 2, we present and discuss results for neat glycerol, the transport of an excess proton in liquid glycerol and an HCl molecule ionizing in glycerol, in section 3. Conclusions are given in section 4.

II. Methods

All ab initio simulations discussed in the present paper were carried out with the Car−Parrinello molecular dynamics method[40] using the code CPMD.[42] In this approach interatomic forces are calculated on the fly at each time step from an electronic structure calculation based on DFT. We employed the so-called BLYP functional consisting of the Becke exchange energy[43] and the correlation energy by Lee, Yang, and Parr.[44] This particular functional has been shown to reproduce the properties of hydrogen bonding systems such as liquid water[45] and liquid ammonia.[46] To describe the interaction between the valence electrons and the nuclei, we used the norm-conserving pseudopotentias developed by Goedecker, Teter, and Hutter.[47] For the plane wave expansion of the valence electron wave functions the cutoff was 70 Rydberg. The time step for the integration of the equations of motion was 0.12 fs and the electron mass was 900 amu. A mass of 2 amu was used for the protons. Although nuclear quantum effects might be of some quantitative importance, particularly for the transport of protons, we treated the dynamics of all nuclei classically.

Initial configurations for the ab initio simulations were generated with the following procedure. First, 16 identical glycerol molecules were placed at random positions with identical orientations in a periodic box of side length 12.46 Å, corresponding to $\rho = 1.261$ g/cm^3,[48] the experimental density of liquid glycerol. Then, the energy of the system was minimized with a combination of the steepest descent and the Newton−Raphson algorithm using the CHARMM code[49] with the charmm27 force field.[50] This program package was employed to carry out all classical force field molecular dynamics simulations used to generate well-equilibrated initial conditions for the ab initio simulations. After the minimization, one of the glycerol molecules was replaced by an HCl molecule with a bond length of 1.27 Å (the bond length of HCl in the gas phase). This configuration was used as the initial condition for a molecular dynamics simulation in which the temperature was continuously raised from 0 to 300 K in 20 ps. To correct for the change in density caused by the removal of the glycerol molecule and the insertion of the HCl molecule, the system was then subjected to a 200 ps force field molecular dynamics simulation in the NPT ensemble at a temperature of 300 K and a pressure of 1 atm. In this simulation the time step was 1 fs and the pressure and temperature were preserved using the extended system method.[51−53] The final box size of 12.45 Å was used in all subsequent simulations of the glycerol−HCl system. After the simulation in the NPT ensemble the system was equilibrated for 400 ps at constant energy with an average kinetic energy corresponding to a temperature of 300 K. All of these simulations were carried out with CHARMM.

The final configuration obtained in the procedure described above was used as initial configuration for the CPMD simulation of an HCl molecule in liquid glycerol. We first equilibrated the system for 4 ps at 300 K with the intramolecular H−Cl distance constrained at 1.27 Å. Then the constraint was released and the system was propagated for another 4 ps during which the HCl dissociated. To generate another, independent dissociation event, the simulation with constrained H−Cl distance was resumed and run for another 0.5 ps. The final configuration of this simulation was then used as the initial configuration of a second 4 ps simulation without intramolecular constraint on the HCl molecule. The results of these simulations are described in detail in section 3.3.

To substantiate the validity of the DFT description of the system, we carried out two further CPMD simulations, one of pure liquid glycerol and one of glycerol plus an excess proton. The initial configurations for these simulations consisting of 16 glycerol molecules in a periodic box with side length 12.46 Å with and without an extra proton were again prepared by placing 16 glycerol at random positions in the simulation box. In the case with the excess proton an extra proton was then placed by hand on one of the glycerol oxygen atoms. The extra charge was evenly distributed on the two hydrogen atoms

attached to this particular same oxygen atom. Both in the case with and without excess proton the configurations were then quenched to a local energy minimum and then equilibrated by running two 1 ns trajectories with the CHARMM code and the charmm27 force field at a temperature of 300 K. Because this force field does not allow chemical bonds to break or to form, the excess proton remained attached to the same oxygen throughout this equilibration run.

The final configurations of these force field simulations were taken as initial configurations for two CPMD equilibrations runs of length 2.9 ps. During the equilibration the system was thermostated by rescaling the particle velocities whenever the instantaneous kinetic energy differed by more than 10% from the target kinetic energy corresponding to an temperature of 300 K. The final configurations of these equilibrations runs served as initial conditions for two constant energy production runs of length 21.5 ps, one with and one without excess proton. Both runs were carried out at energies corresponding to an average temperature of about 300 K. The results of these simulations are described and discussed in sections 3.1 and 3.2.

III. Results and Discussion

A. Neat Glycerol. We first analyzed the results of our 21.5 ps CPMD simulation of 16 glycerol molecules without excess proton in terms of pair correlation functions between different types of atoms. Because, as we will discuss later in more detail, structural reorganizations in liquid glycerol are slow, global molecular reorganizations cannot take place on the time scale of the simulation. Thus, these pair correlations functions bear a strong signature of the initial configuration prepared with force field based molecular dynamics simulations and the results presented in this section must be interpreted with caution.

Intermolecular pair correlation functions involving oxygen and carbon atoms are shown in Figure 1 along with results of the force field simulations of Root and Berne.[22] The potential energy function used in this study was a fully flexible model developed by Root and Stillinger[17] in which CH and CH_2 groups were treated as united atoms. Only hydroxyl hydrogen atoms were treated explicitly. Although for the carbon−carbon pair correlation function the results of ab initio and force field simulations agree well, there are some discrepancies for the oxygen−oxygen and carbon−oxygen pair correlation functions. In particular, the position of the first peaks of $g_{OO}(r)$ and $g_{CO}(r)$ in the CPMD simulation are shifted to shorter distances by a few tenths of an Ångstrom with respect to the force field results. Also, the heights of the peaks differ.

The discrepancies between ab initio and force field results are more pronounced for the intermolecular pair correlation functions involving hydrogen atoms as shown in Figure 2. Due to the importance of the hydroxyl hydrogen atoms for proton transfer, we considered only these hydrogens in this analysis. The strongest deviations from the force field results are observed for the oxygen−hydrogen pair correlation function shown in the central panel of Figure 2. Compared with the results of Root and Berne, the ab initio OH pair correlation function has a considerably sharper and higher peak shifted to shorter distances pointing to stronger hydrogen bonds in the DFT model. Because other force field simulations using an all atom model also yielded a shifted and narrower first peak of $g_{OH}(r)$,[54] these deviations are most likely due to the united atom approximation used in ref 17.

Both in the gas phase and in the liquid state the glycerol molecule can exist in several different conformations. These conformations differ in the two torsional angles spanned by the backbone carbon atoms and the two terminal oxygen atoms.[17,55] Force field simulations[55] indicate that at a temperature of $T =$ 300 K isomerizations between these conformations occur at a rate of about five transitions per molecule and per nanosecond. We have verified that in our CPMD simulation the different conformations occur at approximately the ratios found in the force field simulations of Chelli et al.[55] Furthermore, the number of jumps between different conformations observed during our 21.5 ps CPMD trajectory is consistent with the rates found in ref 55. For a particular molecule, however, the time between transitions is far beyond the simulation time of 21.5 ps such that the relative weight of different conformations observed in the CPMD simulation is most likely a fingerprint of the initial conditions which were generated with force field methods as described in the previous section.

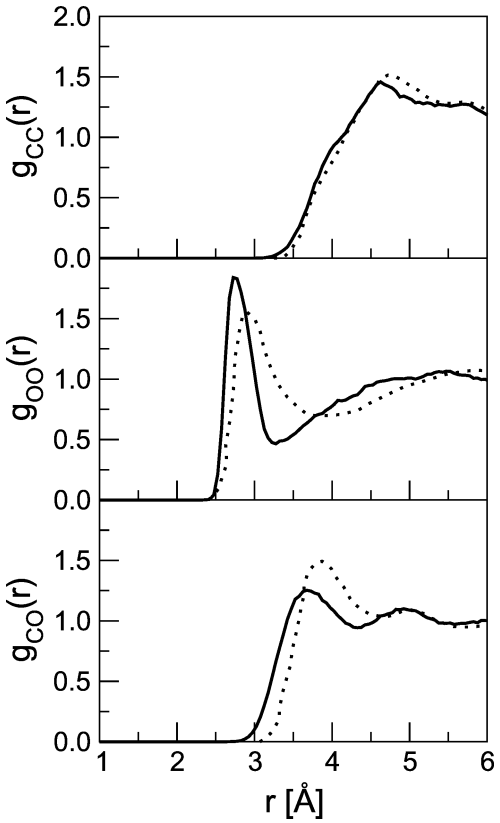

Figure 1. Intermolecular carbon−carbon (CC), oxygen−oxygen (OO), and carbon-oxygen (CO) pair correlation functions (from top to bottom) from our CPMD simulation of 16 glycerol molecules (solid lines) and from a molecular dynamics simulation of 256 glycerol molecules with a classical force field taken from ref 22 (dotted lines).

To assess the dynamical properties of the ab initio glycerol, we have determined the mean squared deviation of the oxygen atoms and of the centers of mass of the glycerol molecules as a function of time (see Figure 3). Both curves show a sharp short time increase corresponding to ballistic motion. After about 0.5 ps both curves reach an approximately linear regime, in which the diffusion constant can be determined from the slope of the curves. The seemingly larger diffusion coefficient of the oxygen atoms is due to rotational motion of the glycerol molecules. Because the rotation of whole molecules takes place on a time scale longer than the simulation time, the rotational contribution to the mean square displacement has not saturated yet, yielding to an apparently larger diffusion constant. Fitting a straight line to the center of mass mean square displacement, shown as a dashed line in Figure 3, in the linear regime (from 1.0 to 10.0 ps) yields a translational diffusion coefficient of

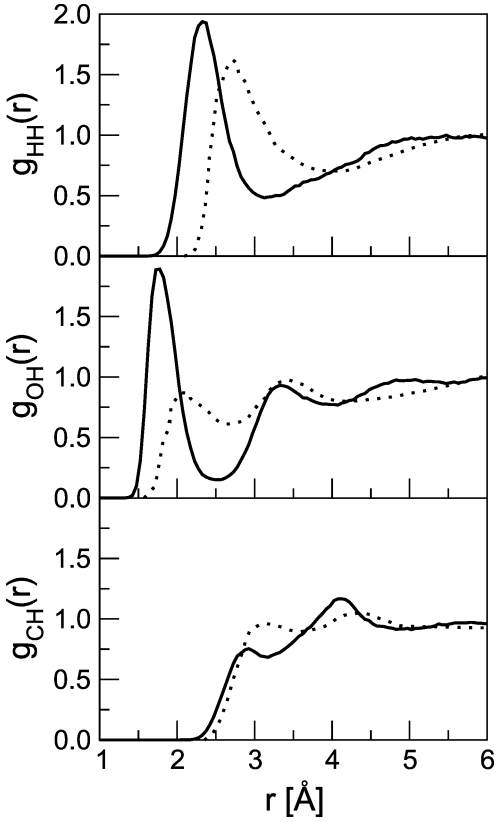

Figure 2. Intermolecular hydrogen−hydrogen (HH), oxygen−hydrogen (OH), and carbon−hydrogen (CH) pair correlation functions (from top to bottom) from our CPMD simulation of 16 glycerol molecules (solid lines) and from a molecular dynamics simulation of 256 glycerol molecules with a classical force field taken from ref 22 (dotted line). Only hydroxide hydrogens were considered in the calculation of these pair correlation functions.

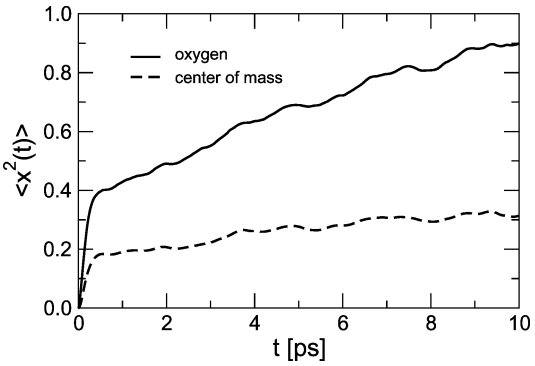

Figure 3. Mean square displacement $\langle[\mathbf{r}(t) - \mathbf{r}(0)]^2\rangle$ of the oxygen atoms (solid line) and of the centers of mass of the glycerol molecules (dotted line) as a function of time obtained from the 21.5 ps CPMD simulation of neat glycerol.

approximately $D_{com} = 2.5 \times 10^{-3}$ Å^2 ps^{-1}. Due to statistical and systematic errors related to the relative shortness of our runs and the small system size this number can be taken only as a rough order of magnitude estimate of the diffusion constant. The diffusion coefficient obtained from our simulation agrees well with the diffusion constant determined in classical force field simulations[55] but exceeds the value found in NMR experiments[24] by about an order of magnitude.

Next, we analyze the ab initio trajectory in terms of hydrogen bonds. Here, an intermolecular hydrogen bond is defined to exist between two OH groups if the distance between the oxygen atoms is less than 3.5 Å and the HOO angle is less than 35°. Intramolecular hydrogen bonds are more strained and an angle

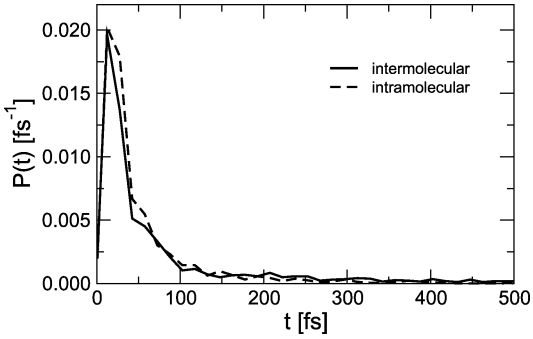

Figure 4. Distribution of lifetimes of intermolecular and intramolecular hydrogen bonds.

of 65° was used for their definition.[22] On the average there were 2.85 intermolecular and 0.40 intramolecular hydrogen bonds per molecule, implying that almost every hydroxyl group is donating and accepting an intermolecular hydrogen bond. On average, each molecule donates nearly three hydrogen bonds to neighboring molecules and accepts the same number of hydrogen bonds from them. The fact that the total number of hydrogen bonds per molecule is larger than 3 points to the existence of so-called bifurcating hydrogen bonds corresponding to hydrogens simultaneously bound to two oxygens.[17] With a more restrictive hydrogen bond definition, however, such bifurcated hydrogen bonds disappear. The average numbers of hydrogen bonds found in our simulation are considerably higher than those found by Root and Berne (1.7 intermolecular and 0.08 intramolecular hydrogen bonds per molecule using an only slightly different hydrogen bond definition),[22] again pointing to the a larger hydrogen bond strength in the DFT description.

To study the dynamics of the hydrogen bond network, we have calculated distributions of hydrogen bond lifetimes depicted in Figure 4. The lifetime of a hydrogen bond is defined as the time interval between the formation of a hydrogen bond and its breaking. This distribution function has a peak at about 15 fs and then decays to zero within 200 fs. The relatively short lifetime is due to fast fluctuations, leading to a temporary disruption of the hydrogen bonds that rapidly re-form in most cases. For this reason the lifetime of a hydrogen bond is very sensitive to the hydrogen bond definition. To characterize the dynamical properties of the hydrogen bonding network in a way more independent of the details of the hydrogen bond definition, we have determined the time correlation function

$$C(t) = \frac{\langle h(0)\, h(t)\rangle}{\langle h(0)\rangle} \tag{1}$$

for the hydrogen bond population operator $h[r(t)]$. The function $C(t)$ measures the conditional probability to observe a hydrogen bond between a particular pair of oxygens at time t provided there existed one at time 0. Here, the function $h[r(t)] = 1$ if there is a hydrogen bond between the pair of tagged oxygens and it vanishes otherwise.[56] This hydrogen bond correlation function has been used before to study hydrogen bond kinetics in liquid water.[56,57] Though the short time behavior of this correlation function strongly depends on the particular hydrogen bond definition, its long time behavior should be largely independent from it.

The correlation function $C(t)$, depicted in Figure 5 for intermolecular hydrogen bonds, displays a sharp drop for short times ($t < 100$ fs) and then slowly decays toward its asymptotic value of $C(t\rightarrow\infty) = \langle h\rangle$, which is of the order of $1/N_O$ where N_O is the number of oxygen molecules. Though the short time

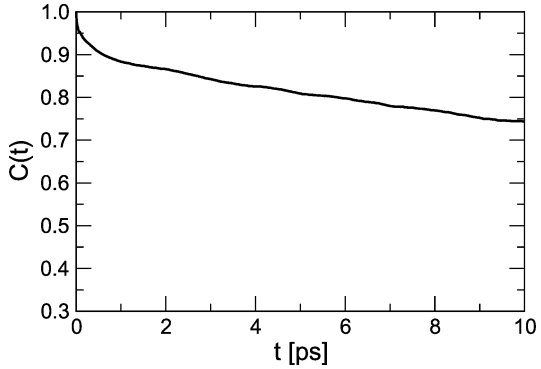

Figure 5. Hydrogen bonding correlation function $C(t)$ for intermolecular hydrogen bonds.

drop is due to temporary breakings of the hydrogen bond, the long time behavior is determined by true hydrogen bond cleavages. At $t = 10$ ps, 70% of the hydrogen bonds present at $t = 0$ still exist. This result is consistent with the force field simulations of Chelli et al.[54] Though the length of our CPMD trajectory is not sufficient for a quantitative analysis of hydrogen bond kinetics, our data indicate that the typical lifetime of a hydrogen bond in liquid glycerol at the thermodynamic conditions studied here exceeds 10 ps by far.

B. Excess Proton in Glycerol. The transport of an excess proton away from the chloride ion following the early events of the HCl dissociation is an important part of the ionization process. Proton transfer occurs via hopping events between hydrogen-bonded hydroxyl groups leading to the diffusion of a charge defect continuously changing composition. In liquid water (and in other hydrogen-bonded liquids), excess protons move in a similar way and this mode of motion is termed the Grotthuss mechanism.[26]

Proton transfer in water and in glycerol differ in an important way. In liquid water, each water molecule accepts and donates two hydrogen bonds in the average. The resulting network of hydrogen bonds percolates through the whole liquid. For a proton hopping along hydrogen bonds from one water molecule to another, each vertex of this network is a branching point with several ways to proceed further. The proton can either move back to the water molecule from which it came or hop on to one of two more neighboring water molecules accepting hydrogen bonds from the water molecule on which the excess charge currently resides.

In liquid glycerol the situation is fundamentally different. Although also in glycerol the hydrogen network percolates through the liquid (each glycerol molecule donates and accepts up to three hydrogen bonds), it does so only if one considers entire glycerol molecules to be the vertices of this network. However, from the viewpoint of proton transfer, Grotthuss-like proton hops do not involve whole glycerol molecules but rather single hydroxyl groups. Only the hydroxyl groups can act as relay stations in the Grotthuss mechanism and therefore they are the relevant units we have to consider. Neglecting bifurcating hydrogen bonds, each hydroxyl group can donate and accept only one hydrogen bond. For this reason the hydrogen bonding network consists of a set of unconnected, one-dimensional chains of hydrogen-bonded hydroxyl groups. These chains offer transfer routes for the excess proton through the liquid. Diffusion of protons over distances longer than the typical length of such one-dimensional chains requires chain breaking and formation of new chains.

In this sense, the hydrogen bonding structure in liquid glycerol is similar to the one in liquid hydrogen fluoride, in which linear chains of hydrogen-bonded HF molecules are known to form.[31] Ab initio simulations[31] have demonstrated that along these hydrogen bond chains, with a typical length of 4−8 monomers, proton motion is rapid with hopping times on the order of 100 fs. Interestingly, the proton is preferentially located at the center of the linear HF chains. This effect, observed also for proton transfer along 1d water chains confined to the interior of narrow pores, is of purely electrostatic origin and can be rationalized with a simple dipole model.[32] As the proton moves along the chain, it flips the dipoles associated with the HF (or water) molecules. The interaction of these flipping dipoles and the moving charge with other dipoles in the chain leads to an effective electrostatic repulsion between the excess charge and the endpoints of the chain. It is this effective interaction that pushes the charge defect to the center of the chain. In liquid HF, protonic diffusion proceeds through connection of the protonated chain to a neutral chain by formation of a new hydrogen bond. The proton then moves to the center of the new chain. When a hydrogen bond of this chain breaks, two new chains form and the proton again moves to the center of its chain. Through a series of such chain reorganizations, which occur on a picosecond time scale, the excess proton can diffuse through the whole liquid. It is well possible that also in liquid glycerol a similar process, in which proton transfer is driven by merging and breaking of one-dimensional hydrogen bond chains, takes place. As we have observed in our simulation, formation of new chains cannot be the only slow process determining the rate for proton diffusion. Even along existing chains proton transfer in liquid glycerol can be slow. Whether this is due to electrostatic effects similar to those observed in single file water chains or is caused by particular hydrogen bonding patterns or the internal conformation of glycerol molecules near the excess charge is currently unknown.

To further study proton transfer in liquid glycerol, we performed a CPMD simulation at 300 K of a system consisting of 16 glycerol molecules and one extra proton initially attached to one of the hydroxyl groups of a glycerol molecule. The procedure used to generate a well equilibrated initial condition for this run is described in section 2. After a further CPMD equilibration run of 3 ps, we followed the time evolution of the system for 21.5 ps.

A quantitative study of the possible protonic solvation structures requires a procedure to determine the position of the excess charge in the simulation box. In ab initio simulations all atoms are treated on the same footing and no a priori information on chemical bonding is available. Hence, the system must be partitioned into molecules using geometric or electronic criteria. To do that, we proceed in the following way: From the positions of the individual atoms we first determine the carbon backbone of the 16 glycerol molecules by using simple distance criteria. Then we assign each oxygen atom to the closest carbon atom. Finally, we assign each hydrogen atom to the closest oxygen or carbon. In this way we obtain 16 molecules, most of which possess 8 protons. One glycerol molecule, however, holds 9 protons instead of 8 and this extra proton is always next to one of the oxygen atoms. We call this particular oxygen atom carrying two hydrogens instead of one the "special oxygen". The position of the special oxygen atom is defined to be the location of the excess charge. Of the two protons assigned to the special oxygen, the one with the larger distance to the special

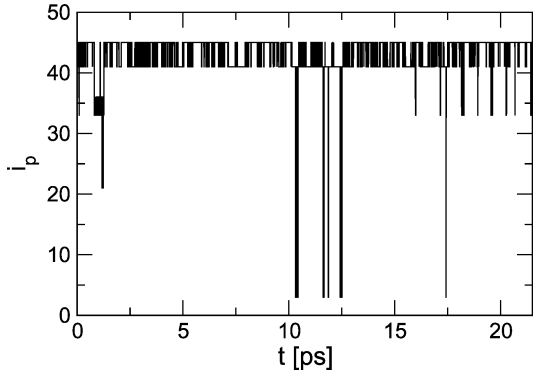

Figure 6. Index of the oxygen carrying the excess proton, the special oxygen, as a function of time.

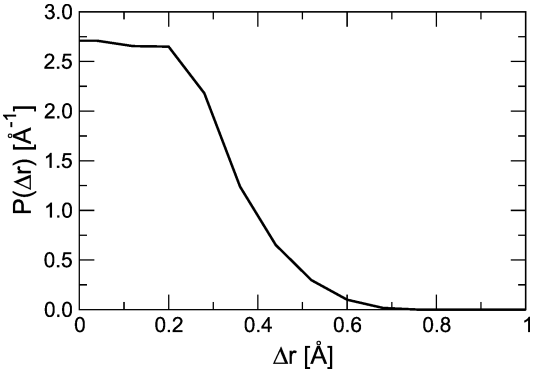

Figure 7. Distribution of the proton-transfer coordinate Δr.

oxygen is defined to be the excess proton. With this definition we can now study the structure and the dynamics of the excess proton.

During the 21.5 ps run the excess charge was located on several different oxygen atoms belonging to different glycerol molecules and 536 hops of the excess proton between these oxygen atoms occurred. During the whole simulation the excess charge was never located on one of the oxygens bound to the central carbon atom but always resided on one of the terminal oxygens. The index of the special oxygen as a function of time is depicted in Figure 6. Most of the time the excess proton oscillates between two oxygen atoms, but at times correlated hops of the charge defect over more than one hydrogen bond occur. Each of the hops shown in this figure is not necessarily associated with a real transfer of the excess proton from one glycerol molecule to the other. Oscillations of the excess proton about its average position in a configuration in which it is shared between two oxygen atoms also lead to a change of the special oxygen and hence to apparent hops of the excess proton from one oxygen to another.

In our CPMD simulation the proton is observed to exist in a continuum of possible configurations between two limiting cases. In one of these limiting configurations the excess proton is bound to a particular oxygen atom of a glycerol molecule. This particular oxygen atom then holds two protons instead of one. In the other limiting configuration two hydroxyl groups share the excess proton, which is located midway between two oxygen atoms. The solvation structures of an excess proton in liquid glycerol bear some similarity with the situation observed in liquid water. In this case, the excess proton can exist in a continuum of structures between the Eigen cation (or $H_9O_4^+$), in which the excess proton is bound to a particular water molecule, and the Zundel cation (or $H_2O_5^+$), in which the excess proton is shared by two water molecules.[36,29] The distribution of the proton-transfer coordinate $\Delta r \equiv |r_2 - r_1|$ obtained from our simulation is shown in Figure 7. Here, r_1 is the distance of the excess proton to the special oxygen and r_2 is the distance of the excess proton to oxygen to which it is hydrogen bonded. The distribution of the coordinate Δr has a broad peak at $\Delta r = 0$, indicating that the configuration with the excess proton shared between two hydroxide groups is the most stable one, but large fluctuations from it are possible.

When the excess proton transfers from one oxygen to another, the distance between these oxygen atoms is about 2.25 Å, considerably smaller than the average distance between two hydrogen-bonded oxygen atoms. According to the central panel of Figure 1 the peak of the intermolecular oxygen−oxygen pair correlation function $g_{OO}(r)$ in pure glycerol is located at $r =$ 2.75 Å and, at 2.25 Å, the oxygen−oxygen pair correlation

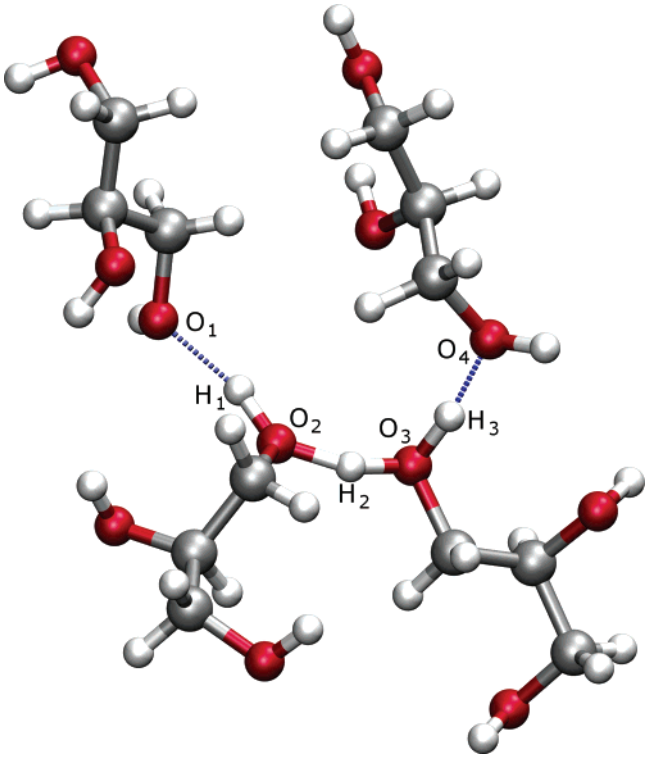

Figure 8. Typical configuration of glycerol molecules around the charge defect. The oxygen denoted by O_3 is the special oxygen and the hydrogen H_2 is the excess proton according to our definition. The oxygen atoms O_1, O_2, O_3, and O_4 are the ones that carry the charge defect in 99% of all configurations sampled in our 21.5 ps CPMD simulation. In more then 96% of all configurations the charge defect is located on oxygens O_2 and O_3. Accordingly, most of the time the excess proton is on hydrogens H_1, H_2, or H_3 with ratios of 1:2:1.

function has decayed to virtually zero. Thus, during the transfer of the excess proton the distance between the two involved oxygen atoms shrinks by about 0.5 Å compared to the equilibrium separation. A similar shortening of the oxygen−oxygen distance during proton transfer has been observed by computer simulations of proton transfer in liquid water.[36,29] In this case the minimum oxygen−oxygen separation is about 2.4 Å, considerably larger than the separation at hopping observed in our simulation.

In our simulation, the proton hops occurred mainly between a small subset of oxygen atoms. The four glycerols predominantly visited during the simulation are pictured in Figure 8 in a typical configuration. In this figure, the excess proton is located between oxygens O_2 and O_3. During the whole simulation run only seven oxygens were visited and for more than 96% of the time the excess proton was located on oxygens O_2 and O_3.

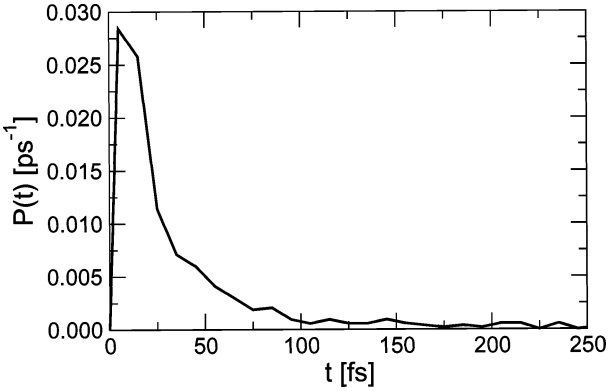

Figure 9. Distribution of permanence times of the proton on a particular oxygen atom.

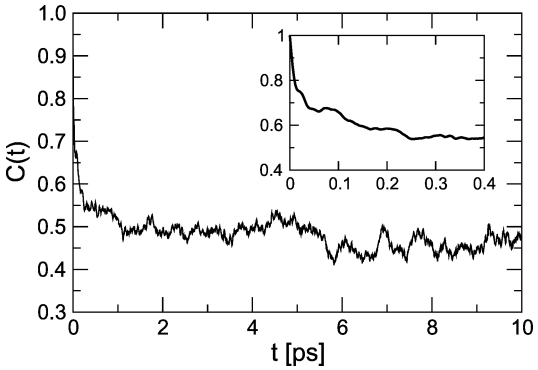

Figure 10. Correlation function $C_p(t)$ for the excess proton. The short time behavior of $C_p(t)$ is shown in the inset.

Similarly, only seven of the 129 protons were the excess proton at one time or another and during more than 98% of the time only three particular hydrogen atoms, H_1, H_2, and H_3 in Figure 8, played the role of the excess proton. This effective confinement of the excess charge is surprising because the hydrogen bond wire available for proton transfer is considerably longer than the segment shown in Figure 8.

Although in our simulation the motion of the proton through the whole system was hindered, transfer between the few oxygens visited during the simulation was facile. On the average, the excess proton is located on a particular oxygen for about 40 fs. The distribution of permanence times, depicted in Figure 9, has a maximum at 20 fs and then decays approximately exponentially with a time constant of about 25 fs. Short permanence times, however, can be caused by short fluctuations that do not necessarily correspond to a true proton hop. A more meaningful analysis consists of calculating the conditional probability $C_p(t)$ to observe the proton on a particular oxygen at time t provided it was located on the same oxygen at time 0:

$$C_p(t) = \frac{\langle h_p(0)\, h_p(t)\rangle}{\langle h_p(0)\rangle} \qquad (2)$$

The indicator function $h_p(t) = 1$ if at time t the proton is on a particular oxygen atom, e.g., oxygen 1, and it vanishes otherwise. In the limit $t \rightarrow \infty$ the correlation function decays to $\langle h_p\rangle = 1/N_O$. In our simulation the charge defect accesses only a small part of the available oxygens and $C_p(t)$ plateaus at a value of $^1/_2$ after a short time (see Figure 10), still much larger than the asymptotic value of $1/N_O = 0.021$. As can be seen in the inset of Figure 10, this decay to the plateau value takes about 100−200 fs.

The mean square displacement of the charge defect, shown in Figure 11 as a function of time, also reflects the effective

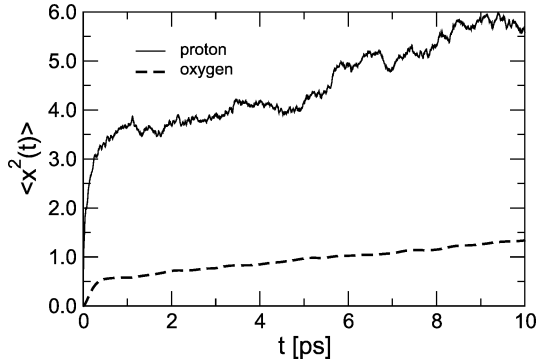

Figure 11. Mean square displacement for the excess proton and for oxygen atoms.

confinement of the charge defect to a small segment of a hydrogen bonding wire. It displays a steep increase for short times ($t < 0.3$ ps) due to the fast hopping of the excess proton along hydrogen bonds but increases much more slowly for longer times. This plateaulike behavior is caused by the effective confinement of the excess proton to a limited portion of the available space. In fact, the diffusion coefficient of the charge defect obtained from the mean square displacement in the linear regime is similar to that of oxygen atoms in the same simulation, but a quantitative comparison is difficult due to the limited statistical accuracy.

Further simulations will be required to study the interplay of proton transfer with the conformational changes of the glycerol molecules and the formation and cleavage of hydrogen bonds. For this purpose, ab initio molecular dynamics simulations at higher temperatures might be useful. At a temperature of $T =$ 400 K, for instance, changes between the different conformations occur at a rate of 35 per molecule and per nanosecond.[55] Although the number of hydrogen bonds available for proton transfer decreases with increasing temperature, at 400 K a considerable number of hydrogen bonds, which form and break at a higher rate compared to lower temperatures, still exists.[55] Thus, at elevated temperatures the processes of interest occur on time scales accessible to Car−Parrinello molecular dynamics simulations.

C. Dissociation of HCl in Glycerol. Starting from different initial conditions we simulated the dynamics of an HCl molecule in glycerol. During both simulations, dissociation occurred followed by rapid proton transfer along the hydrogen bond network. As described in section 2, the starting configurations for these simulations were generated by equilibrating an HCl molecule with a fixed bond length of 1.27 Å for 4 ps. During this equilibration run the constrained HCl molecule donated one hydrogen bond to OH groups of adjacent glycerol molecules and accepted no more than one hydrogen bond from nearby glycerol molecules. Here, a hydrogen bond involving the hydrogen chloride molecule is defined to exist if the Cl−O distance is less than 3.5 Å and the H−O−Cl (or H−Cl−O) angle is less than 30°. A typical configuration of the HCl molecule embedded in liquid glycerol in its typical solvation structure is displayed in Figure 12.

In the early stages after the constraint on the H−Cl distance was released, the proton belonging to the HCl molecule departed from the chloride ion along a hydrogen bond to a nearby oxygen several times. In each case, the proton returned to the chloride ion after less than 30 fs. A typical example of such short time excursions of the proton away from the chloride ion is shown in Figure 13. The distances of the moving proton to the chlorine ion, r_{Cl-H}, and to the accepting oxygen, r_{O-H}, are shown as a

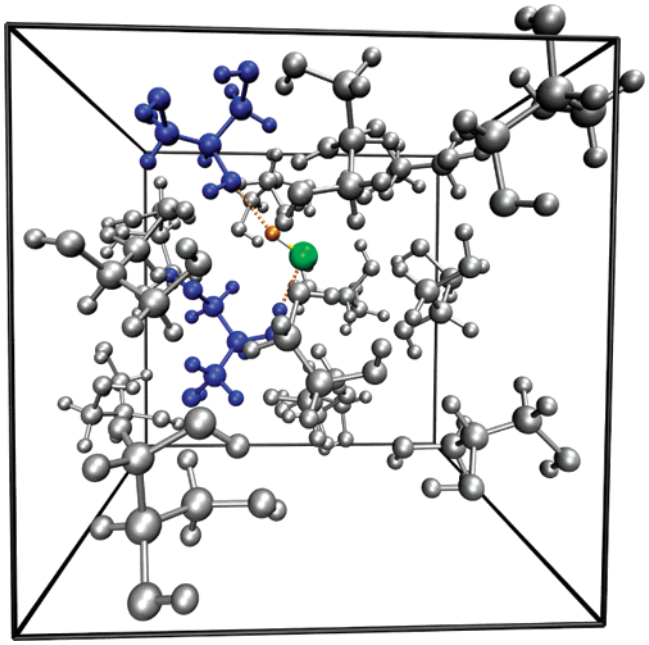

Figure 12. Typical configuration from the Car−Parrinello simulation with constrained H−Cl distance. The Cl atom and the excess proton are shown in green and orange, respectively. The HCl molecule is located at the center of the simulation box. The dark (blue) glycerol molecule are involved in hydrogen bonds (dashed orange lines) to and from the HCl molecule.

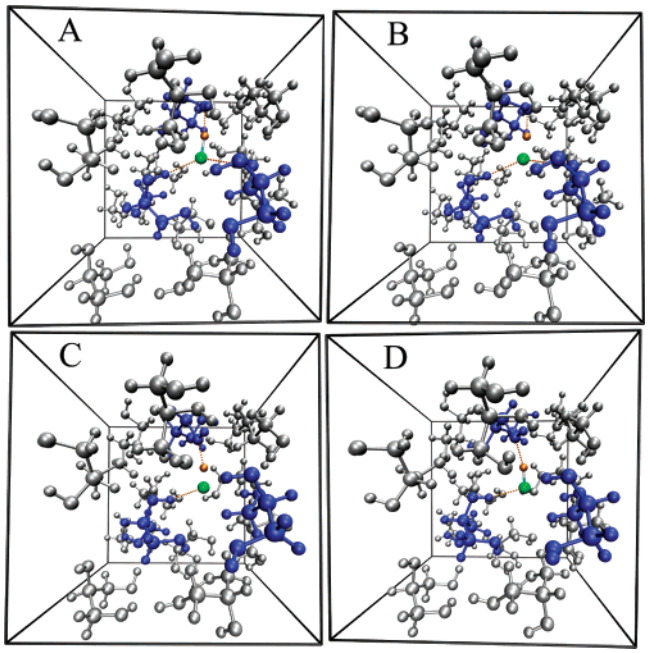

Figure 13. Snapshots from a short dissociation and recombination trajectory. Here the chloride is shown in green and the excess proton in orange. The dark (blue) glycerol molecules are involved in hydrogen bonds (dashed lines) to and from the HCl molecule. After two hydrogen bonds (orange dashed lines) formed to the HCl (A), the HCl dissociated (B). As soon as one of the two hydrogen bonds donated to the chloride ion broke (C), the proton and the chloride recombined (D).

function of time in Figure 14 corresponding to the excursion event depicted in Figure 13. In the example shown in Figure 13, the proton, originally at 1.30 Å from the chloride (Figure 13A), separates from the chloride by as much as 1.83 Å (B) but returns to the chloride after less than 30 fs (C and D). The transient formation of a more stable ion pair (Cl^- and a positively charged glycerol molecule) occurs after the formation

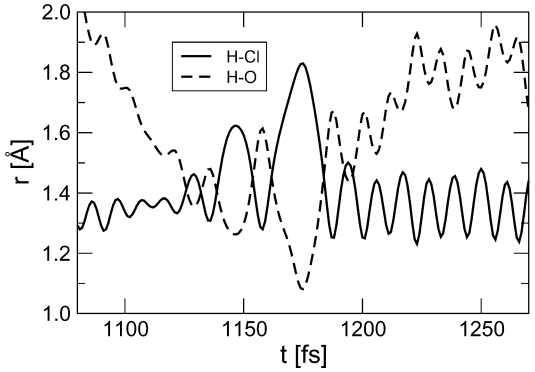

Figure 14. Distances between the proton and the chloride ion (solid line) and between the proton and the accepting oxygen (dashed line) as a function of time along the trajectory shown in Figure 13.

of two hydrogen bonds accepted by the HCl molecule. Once the chloride ion accepts two hydrogen bonds, the proton originally on the chloride can move away from it. This observation is consistent with spectroscopic and theoretical results of Devlin et al.,[6] who found that on ice particles hydrogen chloride can dissociate into a contact ion pair, if it accepts two hydrogen bonds from water molecules on the ice surface.

In the first 2 ps of the trajectory transient separations occurred several times without formation of stable dissociation products. At 2.13 ps, however, the HCl molecule dissociated followed by proton transfer along a ring of 5 hydrogen bonds involving the HCl molecule and 4 OH groups belonging to 4 different glycerol molecules. After 700 fs the excess proton reached the last hydrogen bond of the ring and the excess proton oscillated between the fourth oxygen in the chain and the chloride ion for about 200 fs. Then, the hydrogen bond from the fourth oxygen to the chloride ion broke and the distance of the proton to the chloride ion grew to about 4.3 Å within 300 fs. From this point to the end of the trajectory the excess proton remained in the vicinity of this oxygen hopping only transiently to oxygens nearby. Snapshots of this dissociation process are shown in Figure 15.

To generate another dissociation example, we continued the CPMD simulation with constrained Cl−H distance starting from the final point of the first simulation with constraint described above. After 0.5 ps we released the constraint and followed the time evolution of the system for 4.0 ps. Also along this trajectory the HCl molecule dissociated. After about 2.8 ps the proton separated from the chloride ion and the resulting protonic charge defect quickly moved along a chain of hydrogen bonds to an oxygen atom four hydrogen bonds away from the chloride ion. The charge defect then stayed near this oxygen for the rest of the 4 ps trajectory. In contrast to the first dissociation event, the hydrogen bond chain along which the proton transferred was linear rather than cyclic. Interestingly, dissociation did not occur along a 3 ps trajectory started at the same initial configuration as the first dissociation trajectory, but at a lower temperature of 275 K.

IV. Conclusion

The dissociation events observed in our simulation are consistent with the notion that HCl ionization can occur only if the HCl molecule is coordinated by at least three hydrogen bonds (two accepted and one donated by the hydrogen chloride molecule).[8−10]

To summarize, our simulations suggest the following picture for the dissociation of a HCl molecule in liquid glycerol. The dissociation begins when at least 2 hydrogen bonds are accepted

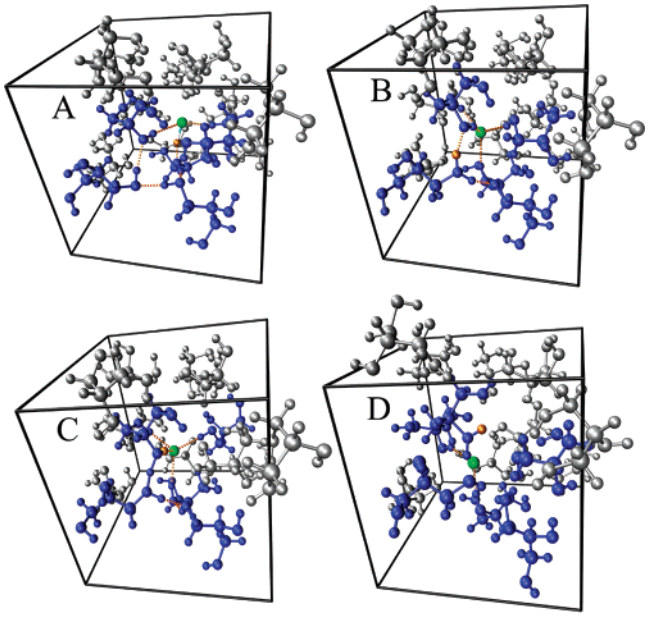

Figure 15. Snapshots along a complete dissociation trajectory. Initially three hydrogen bonds where accepted by the HCl, which was part of a cyclic chain of 4 hydrogen bonds (A). After the HCl dissociated (B), the excess proton (orange) transferred along the hydrogen bond chain to the fourth oxygen (C). Due to the separation of the proton from the chloride (green), the number of hydrogen bonds accepted by the chloride ion increased to four. For about 200 fs the proton oscillated between the fourth oxygen and the chloride ion. Then, the cyclic chain broke and the fourth oxygen and the extra proton moved to a place far away from the chloride (D) where the extra proton continued to oscillate between the fourth oxygen and an oxygen nearby. The dark (blue) glycerol molecules are those involved in the cyclic hydrogen bond chain along which the proton transfers.

by the chloride and the proton is involved in a hydrogen bond to an OH group of a neighboring glycerol molecule. If at the same time a sufficiently long chain of hydrogen bonds away from the chloride is available, the HCl proton can separate from the chloride. When such an ion pair forms, the protonic charge defect is rather mobile oscillating between the first and second oxygen along the hydrogen bond chain. If another hydrogen bond forms to the chloride, the protonic defect separates completely from the chloride. In our simulations the proton never went beyond the fourth oxygen along the hydrogen bond chain, but the reason for this behavior is unclear.

A similar effective confinement of the protonic defect to parts of a hydrogen bond chain was observed in our ab initio simulation of an excess proton in liquid glycerol. The detailed mechanism preventing the excess proton from diffusing freely along the available hydrogen bond chain on the time scale of the simulation remains unclear. To determine whether the proton is trapped by the local conformations of the glycerol molecules around the excess proton, particular hydrogen bonding patterns, or interactions with the hydrogen bond wires along which the protons diffuse more simulations, are necessary. Due to the glassy dynamics of liquid glycerol close to the freezing point, such simulations might be best performed at higher temperature, at which the hydrogen bonding network still exists, but formation and cleavage of hydrogen bonds as well as isomerizations of glycerol molecules occur at a higher rate. The interplay between the kinetics of inter- and intramolecular hydrogen bonds, conformational changes of glycerol molecules and proton transport in liquid glycerol is an interesting subject for future studies.

Due to the high cost of ab initio simulation, we could only study a system of limited size over short time periods. The resulting two dissociation events can only indicate possible scenarios. Future studies will be directed toward a more systematic and statistically exhaustive study of the HCl dissociation process and of the transport of an excess proton in liquid glycerol. To make contact with results of the molecular beam experiments mentioned in the Introduction, it will be necessary to apply ab initio simulation methodologies to study the behavior of HCl at and near the surface of glycerol. Work in this direction is underway in our laboratory.

Acknowledgment. We thank A. H. Muenter and G. M. Nathanson for useful discussions. This work was supported by the Austrian Science Fund (FWF) under Grant No. P17178-N02.

References and Notes

(1) Molina, M. J. *Pure Appl. Chem.* **1996**, *68*, 174−1756.
(2) Molina, M. J.; in *Nobel Lectures, Chemistry 1991−1995*; World Scientific Publishing: Singapore 1997.
(3) Laasonen, K.; Klein, M. L. *J. Am. Chem. Soc.* **1994**, *116*, 11620.
(4) Laasonen, K.; Klein, M. L. *J. Phys. Chem. B* **1997**, *101*, 98.
(5) Ando, K.; Hynes, J. T. *J. Phys. Chem. B* **1997**, *101*, 10464.
(6) Devlin, J. P.; Uras, N.; Sadlej, J.; Buch, V. *Nature* **2002**, *417*, 269.
(7) Packer, M. J.; Clary, D. C. *J. Phys. Chem.* **1995**, *99*, 14323.
(8) Re, S.; Osamura, Y.; Suzuki, Y.; Schaefer, H. F., III. *J. Chem. Phys.* **1998**, *109*, 973.
(9) Chaban, G. M.; Gerber, R. B.; Janda, K. C. *J. Phys. Chem. A* **2000**, *105*, 8323.
(10) Svanberg, M.; Pettersson, J.; Bolton, K. *J. Phys. Chem. A* **2000**, *104*, 5787.
(11) Robertson, S. H.; Clary, D. C. *Faraday Discuss.* **1995**, *100*, 309.
(12) Gertner, B. J.; Hynes, J. T. *Faraday Discuss.* **1998**, *110*, 301.
(13) Allouche, A.; Couturier-Tamburelli, I.; Chiavassa, T. *J. Phys. Chem. B* **2000**, *104*, 1497.
(14) Mantz, Y. A.; Geiger, F. M.; Molina, L. T.; Molina, M. J.; Trout, B. L. *Chem. Phys. Lett.* **2001**, *348*, 285.
(15) Ringeisen, B. R.; Muenter, A. H.; Nathanson, G. M. *J. Phys. Chem. B* **2002**, *106*, 4988.
(16) Ringeisen, B. R.; Muenter, A. H.; Nathanson, G. M. *J. Phys. Chem. B* **2002**, *106*, 4999.
(17) Root, L. J.; Stillinger, F. H. *J. Chem. Phys.* **1989**, *90*, 1200.
(18) Grubbs, W. T.; MacPhail, R. A. *J. Chem. Phys.* **1994**, *100*, 2561.
(19) Wuttke, J.; Hernandez, J.; Li, G.; Coddens, G.; Cummins, H. Z.; Fujara, F.; Petry, W.; Sillescu, H. *Phys. Rev. Lett.* **1994**, *72*, 3052.
(20) Mazur, P. *Science* **1970**, *168*, 939.
(21) Reference deleted in proof.
(22) Root, L. J.; Berne, B. J. *J. Chem. Phys.* **1997**, *107*, 4350.
(23) Erdey-Grúz, T.; Majthényi, L.; Nagy-Czakó, I. *Acta Chim. Acad. Sci. Hung.* **1967**, *53*, 29.
(24) Tomlinson, D. J. *Mol. Phys.* **1972**, *25*, 735.
(25) Grotthuss, C. J. T. *Ann. Chim.* **1806**, *58*, 54.
(26) Agmon, N. *Isr. J. Chem.* **1999**, *39*, 493.
(27) Geissler, P. L.; Dellago, C.; Chandler, D.; Hutter, J.; Parrinello, M. *Science* **2001**, *291*, 2121.
(28) Tuckerman, M. E.; Laasonen, K.; Sprik, M.; Parrinello, M. *J. Chem. Phys.* **1995**, *103*, 150.
(29) Marx, D.; Tuckerman, M. E.; Hutter, J.; Parrinello, M. *Nature* **1999**, *397*, 601.
(30) Liu, Y.; Tuckerman, M. E. *J. Phys. Chem. B* **2001**, *105*, 6598.
(31) Kim, D.; Klein, M. L. *J. Am. Chem. Soc.* **1999**, *121*, 11251.
(32) Dellago, C.; Naor, M. M.; Hummer, G. *Phys. Rev. Lett.* **2003**, *90*, 105902.
(33) Chorny, I.; Benjamin, I.; Nathanson, G. M. *J. Phys. Chem. B* **2004**, *108*, 995.
(34) Åquist, J.; Warshel, A. *Chem. Rev.* **1993**, *93*, 2523.
(35) Vuilleumier, R.; Borgis, D. *J. Chem. Phys.* **1999**, *111*, 4251.
(36) Schmitt, U. W.; Voth, G. A. *J. Chem. Phys.* **1999**, *111*, 9361.
(37) Čuma, M.; Schmitt, U. W.; Voth, G. A. *Chem. Phys.* **2000**, *258*, 187.
(38) Čuma, M.; Schmitt, U. W.; Voth, G. A. *J. Phys. Chem. A* **2001**, *105*, 2814.
(39) Parrinello, M. *Comput. Sci. Eng.* **2000**, *2*, 22.
(40) Car, R.; Parrinello, M. *Phys. Rev. Lett.* **1985**, *55*, 2471.
(41) Kuo, I. W.; Mundy, C. J. *Science* **2004**, *303*, 658.
(42) CPMD, Copyright IBM Corp 1990−2001, Copyright MPI für Festkörperforschung Stuttgart 1997−2001.
(43) Becke, A. D. *Phys. Rev. A* **1988**, *38*, 3098.

(44) Lee, C.; Yang, W.; Parr, R. G. *Phys. Rev. B* **1988**, *37*, 785.
(45) Sprik, M.; Hutter, J.; Parrinello, M. *J. Chem. Phys.* **1996**, *105*, 1142.
(46) Diraison, M.; Martina, G. J.; Tuckerman, M. E. *J. Chem. Phys.* **1999**, *111*, 1096.
(47) Goedecker, S.; Teter, M.; Hutter, J. *Phys. Rev. B* **1996**, *54*, 1703.
(48) *CRC Handbook of Chemistry and Physics*, 77th ed.; CRC Press: Boca Raton, FL, 1996.
(49) Brooks, B. R.; Bruccoleri, R. E.; Olafson, B. D.; States, D. J.; Swaminathan, S.; Karplus, M. *J. Comput. Chem.* **1983**, *4*, 18−217.
(50) Foloppe, N.; MacKerell, A. D. *J. Comput. Chem.* **2000**, *21*, 86.
(51) Andersen, H. C. *J. Chem. Phys.* **1980**, *72*, 2384.
(52) Nose, S.; Klein, M. L. *Mol. Phys.* **1983**, *50*, 1055.
(53) Hoover, W. G. *Phys. Rev. A* **1985**, *31*, 1695.
(54) Chelli, R.; Procacci, P.; Cardini, G.; Califano, S. *Phys. Chem. Chem. Phys.* **1999**, *1*, 871.
(55) Chelli, R.; Procacci, P.; Cardini, G.; Califano, S. *Phys. Chem. Chem. Phys.* **1999**, *1*, 879.
(56) Luzar, A.; Chandler, D. *Nature* **1996**, *379*, 55.
(57) Luzar, A.; Chandler, D. *Phys. Rev. Lett.* **1996**, *76*, 928.